



# Formation of aromatics in heavy gasoline and light LCO ends in FCC



Richard Pujro, Marisa Falco, Ulises Sedran\*

Instituto de Investigaciones en Catálisis y Petroquímica INCAPE (FIQ, UNL–CONICET), Santiago del Estero 2654, 3000 Santa Fe, Argentina

## ARTICLE INFO

### Article history:

Received 9 May 2014

Received in revised form

17 September 2014

Accepted 19 September 2014

Available online 22 October 2014

### Keywords:

Aromatics

Decalin

LCO

FCC

Y zeolite

## ABSTRACT

Decalin, a naphthenic bicyclic compound, was reacted over a commercial FCC catalyst in its fresh, equilibrium and three dealuminated forms in order to analyze the formation of aromatic hydrocarbons in the gasoline and LCO cuts, heavy and light ends, respectively. A batch, fluidized bed CREC Riser simulator laboratory reactor was used at 450 °C with short contact times from 1 to 8 s. The dealuminated catalysts showed an activity intermediate between those of the fresh and equilibrium catalysts, which can be correlated to zeolite content and acidity. Also those properties, at least in the range of values observed in this work, seem to be the most important characteristic in controlling the selectivity of the set of reactions. A reaction network was described, where hydrogen transfer reactions are considered to be the most important to form aromatics, a fact which is essentially unavoidable when a bicyclic naphthenic is converted on these catalysts. Aromatic belonged mainly to the gasoline boiling point range and, to a lower extent, to LCO.

© 2014 Elsevier B.V. All rights reserved.

## 1. Introduction

The process of catalytic cracking of hydrocarbons (FCC) is one of the most important and profitable to produce different fuels such as gasoline and middle distillates and petrochemical raw materials in current refineries [1]. The increasing demand for diesel fuel has induced changes in the operating schemes of the FCC units in order to maximize the yield of light cycle oil (LCO, boiling range usually between 180 and 350 °C), which can be blended together with other cuts from various processes to produce diesel fuels.

There exists a particular interest in the composition of LCO, the fuel quality of which depends on the content of paraffins. Thus, the main problem of LCO as a contributor to diesel fuels is the high concentration of aromatic compounds, typically between 50 and 70% [2], which induces a very low cetane index of about 24–28, while commercial fuels indexes are higher than 50 [3,4]. Moreover, sulphur compounds are present at high level [5]. Overall, these issues depend on the crude source, the catalyst and the process conditions.

Even though technological options exist which can lead to upgrading the quality of LCO, such as partial hydrogenation of aromatics and ring opening of naphthenic compounds [6], these may be expensive. However, the versatility of the FCC in processing different types of feedstocks offers opportunities to improve

LCO yield and quality by either modifying operative conditions [7] or using new catalysts which would produce less aromatics [8,9].

FCC catalyst particles are composed of Y zeolite supported on a matrix (active or inactive) together with various additives, fillers and binders. At present, the catalysts are custom made, according to the particular conditions in a refinery (feedstock, technology, production scheme) [10]. Due to the cyclic process between the reducing atmosphere of the reactor at about 500 °C and the oxidizing, steam containing atmosphere at about 700 °C in the regenerator, the catalyst changes drastically from the fresh state to the so-called equilibrium form, due to a strong dealumination process of the zeolite which reduces its unit cell size, thus impacting on chemical composition and acidic properties; moreover, physical properties also change significantly [11].

However, if specific catalysts are to be developed to decrease the concentration of aromatics in the LCO cut, it is necessary to know the mechanisms of formation of these compounds in the cut, and the impact which various factors such as modifications in the structure, acidity and zeolite content of the catalysts, among others, may induce. The formation of aromatic s in the gasoline–LCO border could be evaluated through the conversion of naphthenic compounds [12,13], which are present at significant concentrations in that boiling range and play an important role in some of the reactions taking place in the complex FCC network.

It is the objective of this work to analyze the influence of dealumination in FCC catalysts on the formation of aromatic

\* Corresponding author. Tel.: +54 342 452 8062; fax: +54 342 453 1068.

E-mail addresses: [rpujro@fiq.unl.edu.ar](mailto:rpujro@fiq.unl.edu.ar) (R. Pujro), [mfalco@fiq.unl.edu.ar](mailto:mfalco@fiq.unl.edu.ar) (M. Falco), [usedran@fiq.unl.edu.ar](mailto:usedran@fiq.unl.edu.ar) (U. Sedran).

**Table 1**  
Properties of the catalysts used.

Catalyst	Zeolite			RE content (wt.%)	Specific surface area (m <sup>2</sup> g <sup>-1</sup> )		Acidity (μmol Py g <sup>-1</sup> )					
	UCS (nm)	Load(wt.%)	Si/Al		Matrix	Total	Bronsted (1545 cm <sup>-1</sup> )			Lewis (1450–1460 cm <sup>-1</sup> )		
							150 °C	300 °C	400 °C	150 °C	300 °C	400 °C
F-cat	2.456	22.00	3.50	0.94	92	243	128.5	102.1	76.3	118.1	42.4	36.9
Cat-1	2.437	18.07	8.26	0.80	72	191	14.6	8.9	8.3	16.7	12.9	11.6
Cat-3	2.434	17.71	10.10	0.94	64	181	12.0	11.6	8.9	23.4	13.4	11.2
Cat-5	2.432	17.04	11.80	1.17	62	173	13.3	10.5	5.0	25.2	17.7	9.8
E-cat	2.430	9.83	14.20	0.70	102	162	5.0	5.1	5.0	13.6	11.0	10.9

hydrocarbons in the heavy end of gasoline and light end of LCO in order to generate more information to assist in the formulation of new, more selective FCC catalysts. Decalin, a bicyclic naphthenic, was used as a test reactant in a CREC Riser Simulator laboratory reactor under very short contact times.

## 2. Experimental

The base catalyst was a commercial FCC catalyst designed to maximize the LCO yield in the process; both its fresh (F-cat) and equilibrium (E-cat) forms were used. The fresh catalyst was subjected to hydrothermal treatment with steam at high temperature in order to induce changes in its physical properties and dealuminate the Y zeolite component. Dealumination was performed on a fluidized bed of catalyst with steam in a tubular quartz reactor at 788 °C, and three different severities were used: 1, 3 and 5 h. The catalyst samples were identified according to the steaming time as Cat-1, Cat-3 and Cat-5, respectively.

The assessment of specific surface areas (BET and *t*-plot methods) was performed with N<sub>2</sub> isotherms at 77 K and the zeolite content (wt.%) was determined following the method by Johnson [14]. The zeolite unit cell sizes (UCS) were determined with the ASTM D-3942-91 X-ray diffraction technique, using a Shimadzu XD-1 equipment. The content of rare earths was determined by the inductively coupled plasma (ICP) method, using a Perkin Elmer Optical Emission Spectrometer OPTIMA 2100 DV.

The nature, amount and strength of acidic sites in the different zeolites were determined by means of the FTIR analysis of adsorbed pyridine (Merck, 99.5%) as a probe molecule in a Shimadzu FTIR Prestige-21 equipment. Approximately 100 mg of the zeolite were pressed at 1 t cm<sup>-2</sup> in order to produce self supporting wafers with density 440 g m<sup>-2</sup>, which were then placed into a cell with CaF<sub>2</sub> windows. Samples were initially degassed at 450 °C during 2 h and a background spectrum was collected at room temperature. Pyridine adsorption was performed at room temperature and after successive desorptions at 150, 300 and 400 °C, spectra were recorded at room temperature with a resolution of 4 cm<sup>-1</sup> at pressure of 10<sup>-4</sup> Torr. The amounts of Brønsted and Lewis acid sites were calculated from the integrated absorbance of the bands at 1545 and 1450–1460 cm<sup>-1</sup>, respectively, by means of the integrated molar extinction coefficients, which are considered independent from the catalyst and site strength [15,16].

The experiments of decalin conversion (Sigma-Aldrich C<sub>10</sub>H<sub>18</sub>, ≥99%, *cis*- and *trans*-decahydronaphthalene isomers mixture), boiling point 189–191 °C, were performed in a CREC Riser Simulator reactor, which is a batch, fluidized bed laboratory reactor which closely mimics the conditions of the commercial FCC process [17]. The unit has been described comprehensively elsewhere [18,19]. Reaction times in the experiments were from 1 to 8 s, temperature was 450 °C and catalyst to oil relationship was 1.12. The mass of catalyst was 0.2 g and the volume of decalin injected was 0.2 ml in all the cases. Experiments of purely thermal cracking, with no

catalyst in the reactor, were performed at the same temperature and the longest residence time.

The reaction products were analyzed by on-line standard capillary gas chromatography, using a 30 m long, 250 mm diameter and 0.25 mm film thickness, non-polar, dimethylpolysiloxane column. Product identification was performed with the help of standards and GC-MS analysis. The coke content was assessed by means of a method with temperature-programed oxidation and further methanation of the carbon oxides over a Ni catalyst, quantified with the help of a FID detector [20]. Mass balances (recoveries) closed to more than 94% in all the cases.

## 3. Results and discussion

### 3.1. Catalyst properties

Table 1 shows the most important catalyst properties. It can be seen that the majority of the properties of the fresh catalyst were modified after dealumination, as long as the Si/Al relationship changed, increasing steadily with steaming time. As a consequence, the UCS of the zeolite crystals decreased due to the higher Si content in the zeolite [21]. In this way, the sample which was dealuminated during 5 h showed an UCS close to that of the equilibrium catalyst. The hydrothermal treatment causes the loss of aluminum atoms from the crystalline zeolite network due to the high temperature hydrolysis of the Si–O–Al bonds [22]. These aluminum atoms migrate to positions out of the zeolite structure and are usually designed as extraframework aluminum [23].

In this type of catalysts, micropores are contributed by the zeolite component and mesopores by the matrix and binder components [24,25], but vacancies in the zeolite framework due to dealumination can produce breaks or even partial collapsing of the crystalline material [22]. Matharu et al. [26], who compared Y zeolite dealumination by hydrothermal treatment and ammonium hexafluorosilicate extraction, observed both micro- and mesoporosity in the hydrothermally treated samples, the mesopore volume increasing with the severity of the treatment. These new pores after dealumination, together with similar consequences on the matrix, manifest in the increasing average mesopore size (for example, 8.5 nm in F-cat to 10.7 nm in Cat-3) and the decreasing total specific surface area of the catalysts (Table 1), as also observed by Salman et al. [27].

The partial collapse of the crystalline material is also reflected in the loss of zeolitic material, with the zeolite content decreasing steadily from the fresh to the equilibrium catalyst through the steamed samples, and also in the loss of acidity. As it will be discussed later, particular attention will be given to Brønsted acidity in view of its mechanistic importance. In effect, total acidity (desorption at 150 °C) decreases significantly from the fresh catalyst to the dealuminated and equilibrium samples. It is to be noted, however, that the amounts of acid sites in the dealuminated catalysts do not differ significantly.

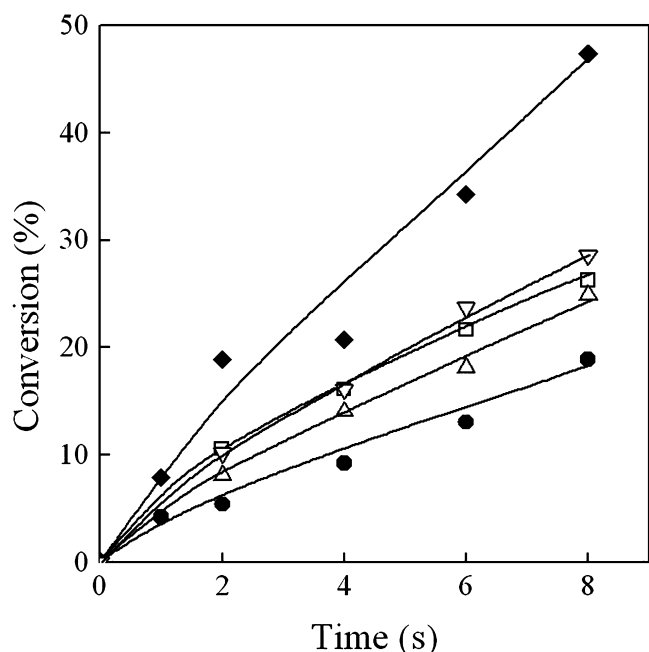


Fig. 1. Conversion of decalin as a function of reaction time. Symbols: (◆) F-cat, (□) Cat-1, (▽) Cat-3, (△) Cat-5, (●) E-cat.

Two periods can be observed during dealumination, UCS, zeolite content and amount of acid sites decreasing much faster during the first hour and then showing a much slower variation, in consistency with previous observations [22].

### 3.2. Catalyst activity

The experiments of purely thermal cracking at 450 °C at the longest contact time showed that conversion was lower than 2%, which was considered negligible as compared to the conversion observed in the catalytic experiments.

Decalin was indeed a mixture of the *cis*- (52%) and *trans*- (48%) configurations. The *cis*-isomer was more reactive, as also noted previously over various FCC catalysts [18]. Different authors also observed this characteristic using different zeolites under a wide range of experimental conditions [28,29]. The conversion of decalin as a function of reaction time is shown in Fig. 1 for the different catalysts; it can be seen that catalyst F-cat is the most active, conversion being two times the values of catalyst E-cat, which is the least active one. The activity of the dealuminated catalysts is intermediate between those of the fresh and equilibrium samples. The conversion profiles of catalysts Cat-1 and Cat-3 are similar, while Cat-5 is less active. By comparing the observed conversions at a given reaction time, the activities of these catalysts can be correlated linearly to their zeolite content (refer to Table 1). Differences in activity among the various catalysts can be considered to be the consequence of dealumination in the zeolite component, which is responsible of activity and selectivity in this type of catalysts [30], impacting significantly on catalyst acidity and zeolite (crystalline material) content, as shown in Table 1. The lowest zeolite content in catalyst E-cat is the consequence of the reaction–regeneration cycles in the commercial unit, and also of the metal contamination by vanadium, particularly, and nickel, which are always present in VGO feedstocks and play a negative role on the catalyst performance [31].

The conversion profiles shown by the dealuminated catalysts are similar, a fact that could be due to the small differences in the amount of crystalline material among them. This is particularly

Table 2  
Product yields (wt.%) in decalin reaction (average conversion 18%).

Products	F-cat	Cat-1	Cat-3	Cat-5	E-cat
C <sub>1</sub> –C <sub>2</sub>	0.14	0.05	0.05	0.05	0.03
C <sub>3</sub>	1.21	0.46	0.50	0.40	0.65
C <sub>4</sub> olefins	0.11	0.08	0.11	0.08	0.15
C <sub>4</sub> paraffins	3.59	1.58	1.63	1.41	0.85
C <sub>5</sub> olefins	0.03	0.02	0.03	0.02	0.06
Cyclopentene	0.01	0.01	0.02	0.01	0.03
C <sub>5</sub> paraffins	1.45	0.71	0.75	0.61	0.66
Cyclopentane	0.14	0.11	0.12	0.10	0.06
C <sub>6</sub> olefins	0.01	0.01	0.01	0.01	0.03
C <sub>6</sub> paraffins	0.73	0.47	0.50	0.43	0.21
C <sub>6</sub> naphthenics	1.71	1.31	1.35	1.29	0.81
Benzene	0.24	0.09	0.08	0.06	0.07
Methylcyclohexene	0.02	0.02	0.02	0.02	0.01
C <sub>7</sub> paraffins	0.14	0.12	0.12	0.11	0.06
C <sub>7</sub> naphthenics	0.80	0.77	0.80	0.77	0.50
Toluene	0.84	0.31	0.30	0.24	0.12
C <sub>8</sub> paraffins	0.12	0.12	0.12	0.13	0.08
C <sub>8</sub> naphthenics	0.28	0.28	0.28	0.30	0.28
C <sub>8</sub> aromatics	0.99	0.40	0.41	0.33	0.15
C <sub>9</sub> paraffins	0.06	0.09	0.07	0.08	0.06
C <sub>9</sub> naphthenics	0.05	0.07	0.06	0.07	0.08
C <sub>9</sub> aromatics	0.85	0.85	0.84	1.05	0.74
C <sub>9</sub> naphthenic-aromatics	0.34	0.68	0.69	0.85	0.95
<i>trans</i> -Decalin	41.03	43.62	43.64	43.55	46.52
<i>cis</i> -Decalin	40.04	40.30	40.25	38.30	34.60
Isobutylcyclohexane	0.15	0.23	0.22	0.30	0.32
3-Butylcyclohexene	0.08	0.13	0.12	0.17	0.19
C <sub>10</sub> aromatics	1.30	2.37	2.46	2.61	4.68
Naphthalene	0.49	0.78	0.62	0.72	0.69
C <sub>10</sub> naphthenic-aromatics	0.43	0.27	0.49	0.46	0.74
Tetralin	0.28	0.44	0.49	0.44	0.60
1,1'-Bicyclopentyl	0.10	0.21	0.19	0.28	0.35
Trimethylbicycloheptane	0.35	0.59	0.56	0.75	0.63
Dimethylbicyclooctane	0.93	1.45	1.04	2.60	2.40
C <sub>11</sub> aromatics	0.03	0.02	0.02	0.11	0.03
Methylnaphthalene	0.09	0.05	0.08	0.07	0.06
C <sub>11</sub> naphthenic-aromatics	0.06	0.04	0.05	0.06	0.06
C <sub>12</sub> <sup>+</sup> aromatics	0.04	0.01	0.02	0.02	0.02
C <sub>12</sub> <sup>+</sup> naphthenic-aromatics	0.01	0.00	0.01	0.01	0.01

true for catalysts Cat-1 and Cat-3, while Cat-5 has less zeolite and consequently is somewhat less active.

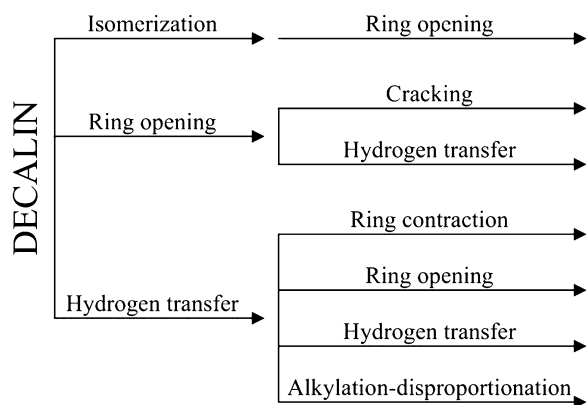
The size of the decalin molecules has been calculated to be slightly smaller than that of the micropores in the zeolite [32]. However, a number of publications showed that the conversion of decalin on Y zeolite is not subjected to diffusion restrictions. In that sense, Mostad et al. [33] compared ZSM-5, offretite, mordenite, different Y zeolites and an amorphous silica-alumina, while Corma et al. [32] reported to ZSM-5, MCM-22, ITQ-2, USY, beta, and MCM-41. Al-Sabawi and de Lasa [34] also compared the performance of Y zeolite with different crystal sizes to conclude that pore diffusion resistance would not affect the overall rate of conversion, in consistency with previous observations by Sousa-Aguiar et al. [35].

It is possible to consider decalin isomers as a single reactant species in the forthcoming yield analysis, based on a large body of evidences about product distributions, kinetics, and isomer reactivities (for example, [28,29,36]).

### 3.3. Reaction products

The set of reactions can be initiated through the electrophilic attack of catalyst surface protons on the tertiary carbons in decalin, as suggested by Sousa-Aguiar et al. [35]; then, activity and selectivity are expected to be directly correlated to the Brønsted sites in the zeolite.

Reaction product hydrocarbons were linear and cyclic olefins and paraffins, bicyclic naphthenics, naphthenic-aromatics, alkylaromatics and diaromatics, comprising the C<sub>1</sub>–C<sub>12</sub> range (Table 2), and thus defining a very complex mixture. This is consistent



**Scheme 1.** Main reactions in the conversion of decalin.

with the wide distribution of acid strengths found in these catalysts (see Table 1). Based on the detailed product identification, reactions which were identified in the decalin conversion network over this type of catalyst were cracking, direct hydrogen transfer, isomerization, ring contraction, ring opening and alkylation–disproportionation [18].

The products can be grouped representing the different reactions promoted by the catalysts, but it is to be noted that different classifications were used by other authors, in response to different analysis of the experimental observations [29,32,34,36]. Cracking reactions are represented by  $C_1$ – $C_9$  compounds (olefins, paraffins, naphthenes, naphtheno-aromatics and aromatics); direct hydrogen transfer by naphthalene and tetralin; isomerization by bicyclic  $C_{10}$  compounds (mainly dimethyl octabicyclic); ring contraction by indane-type compounds; ring opening by  $C_{10}$  alkylated naphthenes and cyclic olefins (such as isobutyl cyclohexane and 3-butyl cyclohexene, respectively) and alkylation–disproportionation can be particularly represented by the yield of  $C_{11}$ – $C_{12}$  alkylated aromatics or naphthenic-aromatics, such as methyl-naphthalene and methyltetralin.

Most of the products were observed at very low conversions and reaction times, thus supporting the concept that reactions such as isomerization, ring opening and hydrogen transfer are simultaneous and occur initially; moreover, reactions that would occur after them in a proposed model [18], such as cracking, ring contraction and alkylation–disproportionation would also take place immediately (Scheme 1). Other authors, who observed small concentrations of aromatics, did not consider that these hydrocarbons can be formed initially; as a consequence, only ring opening was considered a initial reaction at 450 °C [32] or, in systems where hydrogen was present, isomerization and ring contraction [28], or ring opening and contraction [29] were considered initial at 400 °C.

According to the product yields as a function of conversion, cracking reactions were the most important ones over catalyst F-cat, while the other reactions increased their magnitude as long as activity in the catalysts decreased. For example, Fig. 2 shows the product yields of cracking reactions decreasing in the order F-cat, Cat-3 and E-cat, thus defining a ranking which is opposite to that of the product yields of hydrogen transfer reactions; particularly, the product yields of these two reactions are the same over E-cat catalyst. This behavior points again to the controlling effect of the catalysts' zeolite content, and the consequent amount of acid sites, on catalyst activity and reaction network.

Fig. 3 shows the yield curves of the products from the most important reactions (cracking, hydrogen transfer, isomerization and ring contraction) over all the catalysts. It can be seen that they all show a primary character, following the very early occurrence of their products, as also reported by Pujro et al. [18], who

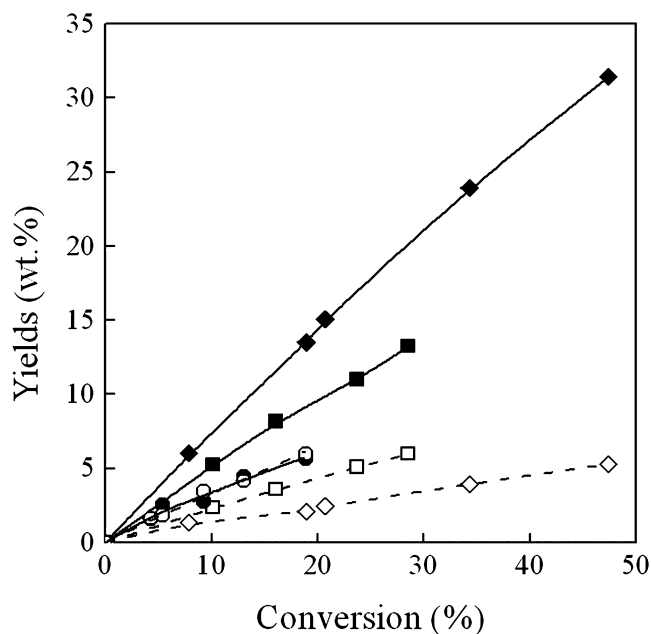
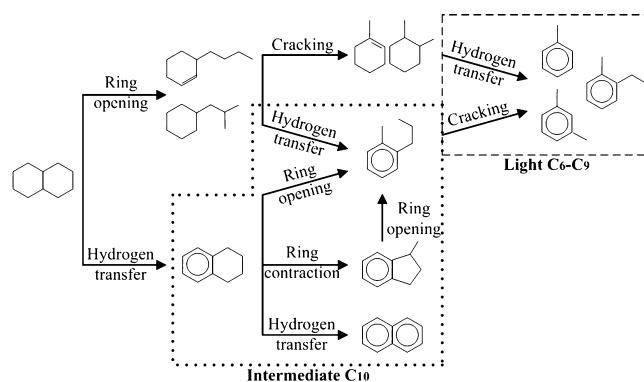


**Fig. 2.** Product yields of cracking and hydrogen transfer reactions as a function of conversion. (◆) F-cat, (■) Cat-3, (●) E-cat. Closed symbols, solid lines: cracking; open symbols, dashed lines: hydrogen transfer.

used prototypes of commercial catalysts. The primary character of the products and reactions can be assigned in view of the linear relationship between yield and conversion, while a secondary character would be revealed by a zero slope at initial conversion.

The yield of products from ring opening and alkylation–disproportionation reactions were always lower than 1% (results not shown), but it was possible to clearly identify their secondary character. These facts contribute to assume alkylation–disproportionation reactions as consecutive to direct hydrogen transfer (Scheme 1). Ring opening products are subjected to other reactions, such as cracking and hydrogen transfer (Scheme 1), due to their high reactivity. Scheme 2 is an example of the reaction network which can lead to the production of aromatic compounds from ring opening and hydrogen transfer reactions, in both the light  $C_6$ – $C_9$  and intermediate  $C_{10}$  range.

The product yields of cracking, hydrogen transfer and ring contraction reactions on dealuminated catalysts (Fig. 3A, B and D) are between those of the fresh and equilibrium catalysts, in accordance to the observed activities (Fig. 1), while the product yield of isomerization reactions over E-cat is very close to those of the dealuminated catalysts (Fig. 3C), a fact which could be due to the similar zeolite load and acid amount in those samples.



**Scheme 2.** Formation of light  $C_6$ – $C_9$  and intermediate  $C_{10}$  aromatics.

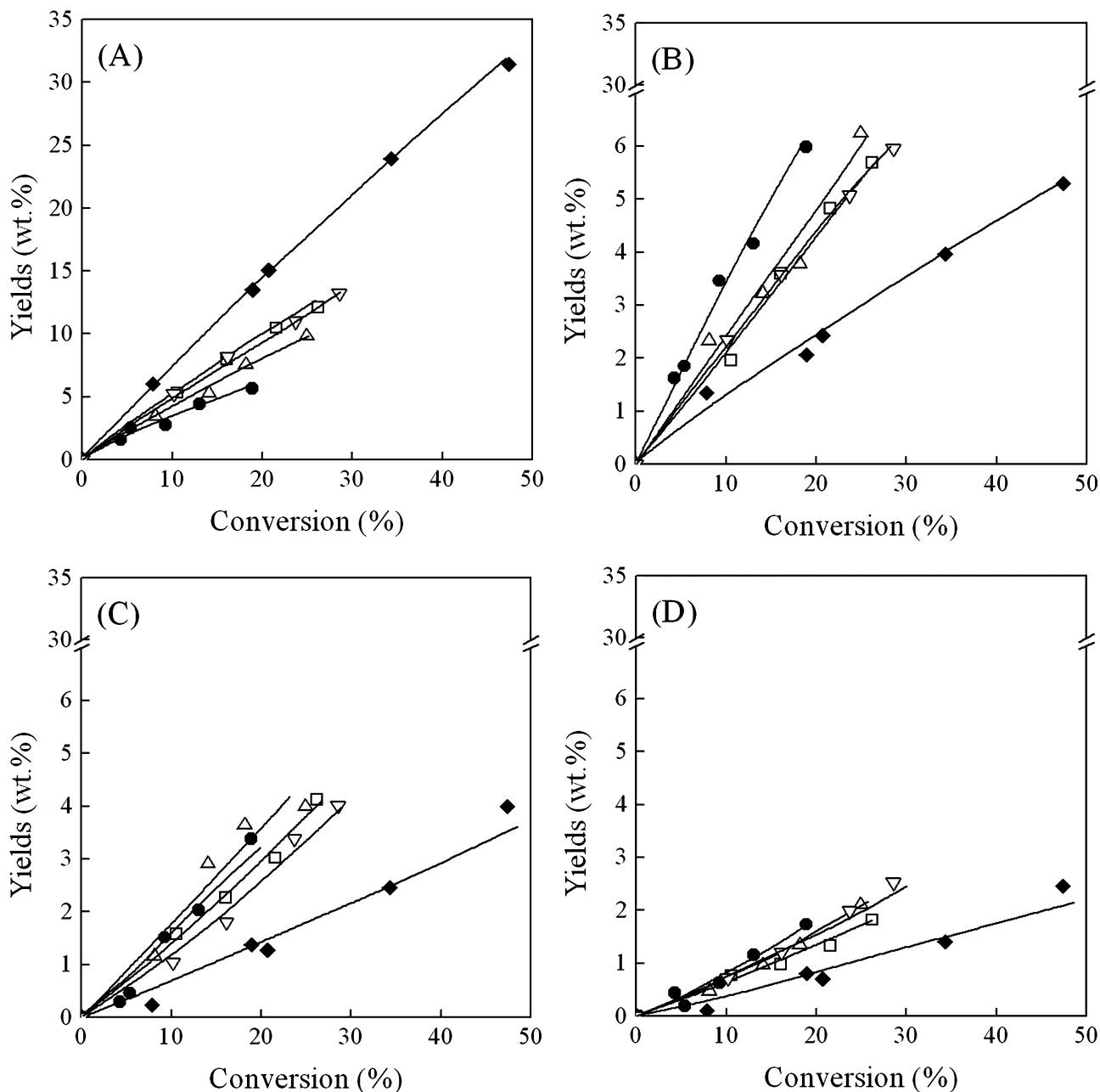


**Fig. 3.** Yield curves for the different reactions. (A) cracking, (B) hydrogen transfer, (C) isomerization, (D) ring contraction. Symbols: (◆) F-cat, (□) Cat-1, (▽) Cat-3, (Δ) Cat-5, (●) E-cat.

A brief analysis in relation to the type of hydrocarbons observed can provide additional information about the mechanisms leading to the formation of aromatics from bicyclic naphthenics in the gasoline (heavy end) and LCO (light end) cuts, showing that aromatic compounds are the most important over all the catalysts, with olefins being the less favored and paraffins and naphthenics showing intermediate values which, moreover, are very similar for the dealuminated catalysts. Fig. 4 shows the yields for each of these groups over the five catalysts. Some evidences are that the yield of olefins and paraffins, which are the main consequence of cracking reactions [18], decrease together with catalyst activities (Fig. 4A and B), with the exception of the yield of olefins over E-cat, which is slightly higher than those of the dealuminated catalysts. On the contrary, the yields of naphthenics, as the consequence of isomerization (leading to bicyclic saturated compounds) and ring opening (leading to alkylated naphthenics) initial reactions, and

further cracking reactions, are all very similar for the dealuminated and equilibrium catalysts (Fig. 4C). Fig. 4D shows that even though the activity of the catalyst decreases, the yield of aromatics increases, being the consequence of hydrogen transfer reactions on naphthenic compounds (Scheme 2).

The previous analysis shows that the dealumination process does not impact in a negative way on the formation of aromatics from bicyclic naphthenics in the range under study, as the change in the zeolite unit cell size and the loss of acidic sites might suggest (Table 1) [13,38]. The higher Si/Al relationship and the lower UCS of the dealuminated catalysts are in line with a decrease in the density of paired acid sites in the zeolite [38], which control bimolecular hydrogen transfer reactions.

This observation could be associated to the characteristics of the model compound, a bicyclic naphthenic, where one of the rings could be continuously susceptible to act as a donor in hydrogen

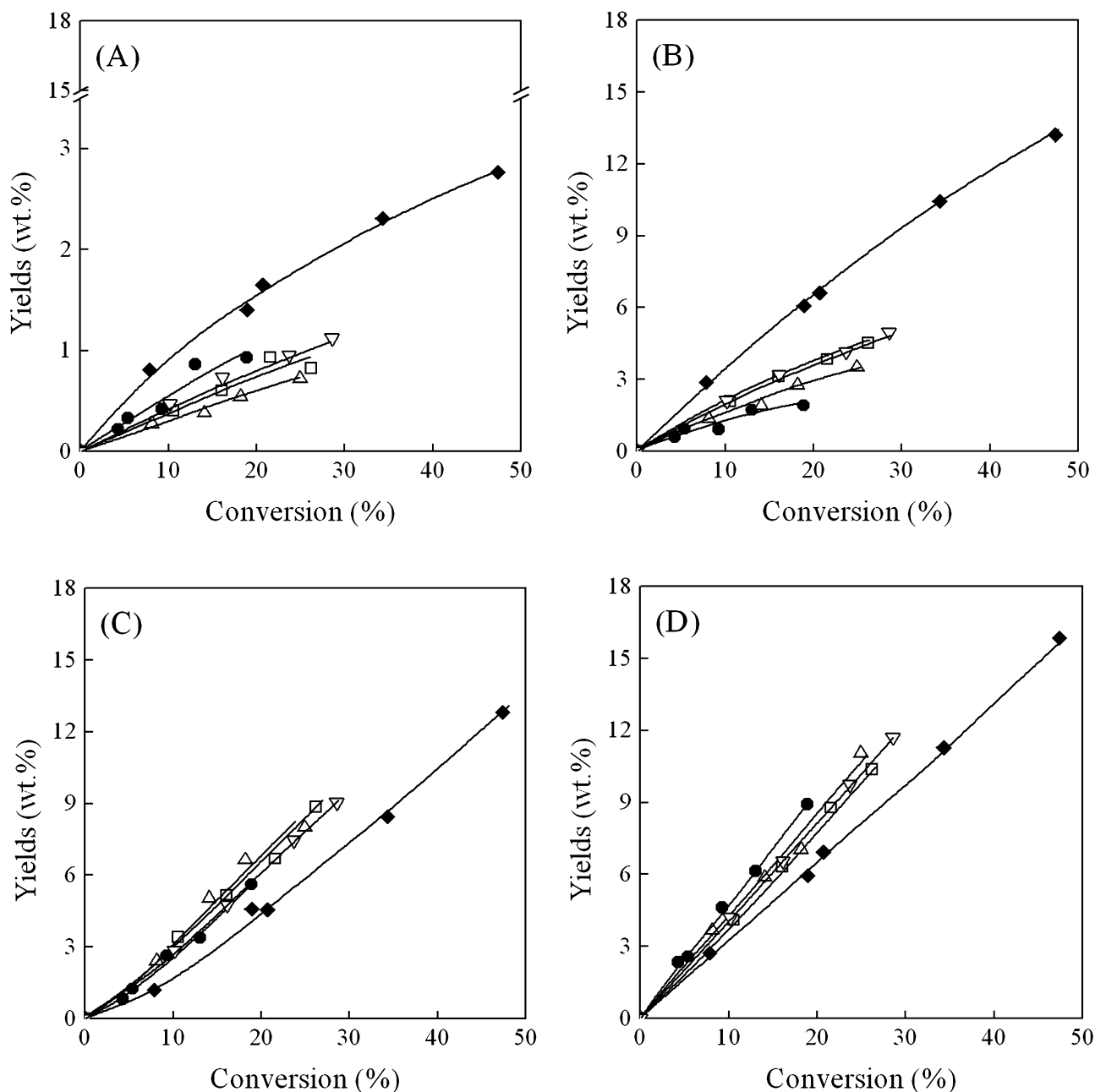


Fig. 4. Yield curves of hydrocarbon groups. (A) olefins, (B) paraffins, (C) naphthenics, (D) aromatics. Symbols as in Fig. 3.

transfer reactions and the other ring subjected to the other reactions (ring opening and contraction). Opening both rings in decalin would not be feasible, or would proceed to a low extension on these catalysts, since no linear  $C_{10}$  paraffins or olefins were observed, and the yields of  $C_7$ – $C_9$  paraffins were also very low. Then, the formation of aromatics would be always present, and even increasing, regardless of the dealumination process which decreases the density of paired acid sites in the zeolite. The degree of site isolation, however, would not be enough to interfere with hydrogen transfer reactions; moreover, the catalysts lose activity due to the loss of crystalline material and reduce the yield of products from cracking.

Aromatic hydrocarbons can be grouped into light  $C_6$ – $C_9$ , intermediate  $C_{10}$  and heavy  $C_{11}^+$  molecular weight compounds. The higher incidence of catalyst activity, particularly on cracking reactions, can be observed on catalyst Cat-F, which favors the formation of light aromatics (Scheme 2). Intermediate  $C_{10}$  aromatics are

preponderant on the dealuminated and equilibrium catalysts and, in all the cases, heavy  $C_{11}^+$  aromatics are formed only in small amounts (yields lower than 1 wt.%). Fig. 5 shows these facts. Light  $C_6$ – $C_9$  aromatics yields decrease as long as the catalysts are less active (Fig. 5A), as well as cracking reactions also decrease (Fig. 3A). On the contrary, the yields of intermediate  $C_{10}$  aromatics increase if the catalyst activity decreases (Fig. 5B).

In relation to the formation of aromatics (most important reactions are shown in Scheme 2), it can be concluded that a more active catalyst would promote the formation of light naphthenic compounds by way of the upper branch in the scheme, finally leading to light aromatics through hydrogen transfer reactions (example of catalyst F-cat). As long as the catalysts are less active, light compounds from cracking decrease their yields, and the bottom branch in the scheme becomes more important, leading to intermediate  $C_{10}$  aromatics.

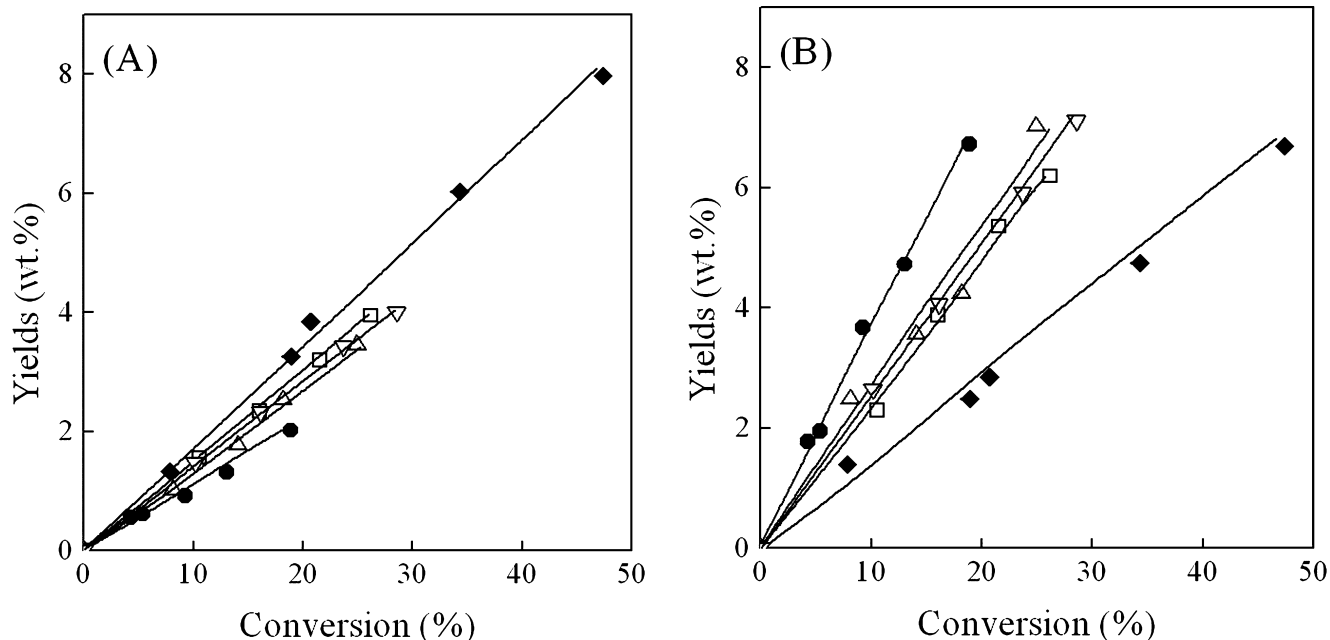


Fig. 5. Yield curves of aromatic hydrocarbons. (A) C<sub>6</sub>–C<sub>9</sub>, (B) C<sub>10</sub>. Symbols as in Fig. 3.

All the catalysts showed that the species with a single ring are the preferred ones among the aromatic products (more than 90%) from intermediate bicyclic naphthenic compounds, in coincidence with reports by Mostad et al. [36] and Al-Sabawi and de Lasa [34].

Coke yields are not too high. In effect, it can be seen in Fig. 6 that the most active catalyst showed a 3 wt.% yield, while for all the other catalysts, they were lower than 1 wt.%, a fact also observed by Al-Sabawi and de Lasa [34], who converted decalin over Y zeolite with different crystal sizes at 550 °C, and by Corma et al. (dcalin on USY zeolite) at 450 °C [32], and by Corma and Ortega (dcalin over a commercial low rare earth USY FCC catalyst) at 400 °C [37].

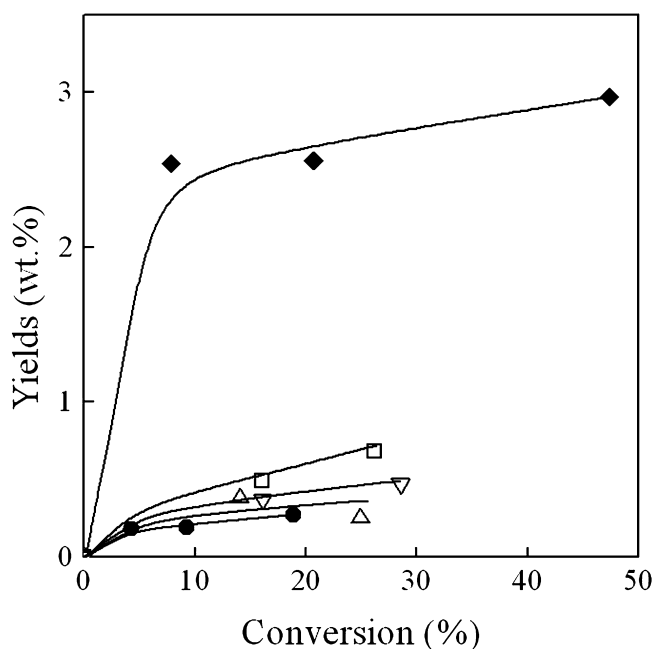


Fig. 6. Coke yield curves. Symbols as in Fig. 3.

#### 4. Conclusions

The hydrothermal dealumination of a commercial FCC catalyst produces important changes in the crystalline structure of the Y zeolite component, which are very fast at short contact times in the steaming method. These dealuminated catalysts showed an intermediate activity between the fresh and equilibrium catalysts, which can be correlated to zeolite content and total acidity; moreover, their conversion profiles were very similar.

The conversion of decalin as a test reactant allowed defining the relative importance of the different reactions occurring on these FCC catalysts that differ in their most important properties such as zeolite content, acidity and unit cell size. The reactions that could be identified were cracking, hydrogen transfer, isomerization, ring contraction, ring opening and alkylation–disproportionation.

The content of zeolite and the amount of acidic sites, at least in the range of values observed in this work, seems to be the most important characteristic controlling the selectivity of the reactions. Among the most important reactions, the lower the zeolite content and the acidity, the lower the selectivity to cracking products.

The occurrence of hydrogen transfer reactions is essentially unavoidable when a bicyclic naphthenic is converted on this type of catalysts under FCC conditions, and lead to an elevated concentration of aromatic compounds which belong mainly to the gasoline boiling point range and, to a lower extent, to LCO. The dealumination of the catalysts and consequent decrease in the zeolite unit cell size up to the levels shown in this work is not enough to interfere seriously with hydrogen transfer.

In order to minimize the yield of aromatics from bicyclic naphthenic hydrocarbons, a relatively more active catalyst (higher zeolite content) is convenient. Alternatively, and considering the usual performance of commercial catalysts in the FCC units, higher stability in the zeolite component would be desirable, or a higher make-up rate needed.

#### Acknowledgements

This work was performed with the financial assistance of National University of Litoral (UNL), Secretary of Science and

Technology (Santa Fe, Argentina) (CAID 2011 no. 501 201101 00329 LI); CONICET (PIP 1257/09) and the National Agency for Scientific and Technological Promotion (PICT 2010/2123).

## References

- [1] P. O'Connor, *Stud. Surf. Sci. Catal.* 166 (2007) 227–251.
- [2] UOP LLC, Diesel Fuel. Specifications and Demands for the 21st Century, UOP LLC, Des Plaines, IL, 1998.
- [3] B.H. Cooper, B.B.L. Donniss, *Appl. Catal., A: Gen.* 137 (1996) 203–223.
- [4] Directive 2009/30/EC of the European Parliament and of the Council, *OJ L140*, 2009, 88–113.
- [5] Ch. Song, X. Ma, *Appl. Catal., B: Environ.* 41 (2003) 207–238.
- [6] V. Calemma, R. Giardino, M. Ferrari, *Fuel Process. Technol.* 91 (2010) 770–776.
- [7] R. Torchio de Oliveira, *Anales IV Encuentro Sudamericano de Craqueo Catalítico, Manaus, Brasil, 2000*, pp. 101–108.
- [8] A. Corma, C. Martínez, L. Sauvanaud, *Catal. Today* 127 (2007) 3–16.
- [9] W.R. Gilbert, E. Morgado Jr., M.A.S. de Abreu, G. de la Puente, F. Passamonti, U. Sedran, *Fuel Process. Technol.* 92 (2011) 2235–2240.
- [10] H.L. Hoffman, *Hydrocarbon Process.* February (1990) 53–54.
- [11] B. Behera, S.S. Ray, *Catal. Today* 141 (2009) 195–204.
- [12] A. Corma, F. Mocholi, V. Orchilles, G.S. Koermer, R.J. Madon, *Appl. Catal.* 67 (1991) 307–324.
- [13] G. de la Puente, U. Sedran, *Appl. Catal., A: Gen.* 144 (1996) 147–158.
- [14] M.F.L. Johnson, *J. Catal.* 52 (1978) 425–431.
- [15] C.A. Emeis, *J. Catal.* 141 (1993) 347–354.
- [16] M.S. Renzini, U. Sedran, L.B. Pierella, *J. Anal. Appl. Pyrolysis* 86 (2009) 215–220.
- [17] H.I. de Lasa, US Patent 5,102,628, 1992.
- [18] R.A. Pujro, M.G. Falco, A.M. Garrido Pedrosa, M.J.B. Souza, E. Morgado Jr., U. Sedran, *J. Braz. Chem. Soc.* 23 (2012) 1378–1387.
- [19] F. Passamonti, G. de la Puente, E. Morgado Jr., W. Gilbert, U. Sedran, *Chem. Eng. J.* 183 (2012) 433–447.
- [20] S.C. Fung, C.A. Querini, *J. Catal.* 138 (1992) 240–254.
- [21] J. Scherzer, *Catal. Rev. Sci. Eng.* 31 (1989) 215–354.
- [22] Q.L. Wang, G. Giannetto, M. Torrealba, G. Perot, C. Kappenstein, M. Guisnet, *J. Catal.* 130 (1991) 459–470.
- [23] C. Marcilly, *Arabian J. Sci. Eng.* 21 (1996) 297–312.
- [24] P. Schneider, *Appl. Catal., A: Gen.* 129 (1995) 157–165.
- [25] Y.Y. Agámez Pertuz, L.A. Oviedo Aguiar, U. Navarro Uribe, M.A. Centeno, J.A. Odriozola, *Rev. Colomb. Quim.* 35 (2006) 7–17.
- [26] A.P. Matharu, L.F. Gladden, S.W. Carr, *Stud. Surf. Sci. Catal.* 94 (1995) 147–154.
- [27] N. Salman, C.H. Rüschler, J.-Chr. Buhl, W. Lutz, H. Toufar, M. Stöcker, *Microporous Mesoporous Mater.* 90 (2006) 339–346.
- [28] D. Kubička, N. Kumar, P. Mäki-Arvela, M. Tiitta, V. Niemi, T. Salmi, D. Yu Murzin, *J. Catal.* 222 (2004) 65–79.
- [29] M. Santikunaporn, J.E. Herrera, S. Jongpatiwut, D.E. Resasco, W.E. Alvarez, E.L. Soghrue, *J. Catal.* 228 (2004) 100–113.
- [30] J. Scherzer, *Stud. Surf. Sci. Catal.* 76 (1993) 145–182.
- [31] S.-J. Yang, Y.-W. Chen, *Zeolites* 15 (1995) 77–82.
- [32] A. Corma, V. González-Alfaro, A.V. Orchilles, *J. Catal.* 200 (2001) 34–44.
- [33] H.B. Mostad, T.U. Riis, O.H. Ellestad, *Appl. Catal.* 58 (1990) 105–117.
- [34] M. Al-Sabawi, H. de Lasa, *Chem. Eng. Sci.* 65 (2010) 626–644.
- [35] E.F. Sousa-Aguiar, C.J.A. Mota, M.L.M. Valle, M.P. da Silva, D.F. da Silva, *J. Mol. Catal.* 104 (1996) 267–271.
- [36] H.B. Mostad, T.U. Riis, O.H. Ellestad, *Appl. Catal.* 63 (1990) 345–364.
- [37] A. Corma, F.J. Ortega, *J. Catal.* 233 (2005) 257–265.
- [38] G. de la Puente, U. Sedran, *Chem. Eng. Sci.* 55 (2000) 759–765.